Molecular Biology of the Cell
Vol. 21, 3125–3136, September 15, 2010

Proteasome Nuclear Import Mediated by Arc3 Can Influence Efficient DNA Damage Repair and Mitosis in Schizosaccharomyces Pombe

Rodrigo Cabrera,*†‡ Zhe Sha,*†‡ Tegy J. Vadakkan,§ Joel Otero,†‖ Franziska Kriegenburg,¶ Rasmus Hartmann-Petersen,¶ Mary E. Dickinson,§ and Eric C. Chang*†

*Department of Molecular and Cellular Biology, §Department of Molecular Physiology and Biophysics, ‖Interdepartmental Program of Cell and Molecular Biology, and †Lester and Sue Smith Breast Center, Baylor College of Medicine, Houston, TX 77030; and ¶Department of Biology, Section for Biomolecular Sciences, University of Copenhagen, DK-2200 Copenhagen, Denmark

Submitted June 11, 2010; Revised July 19, 2010; Accepted July 21, 2010
Monitoring Editor: William P. Tansey

Proteasomes must remove regulatory molecules and abnormal proteins throughout the cell, but how proteasomes can do so efficiently remains unclear. We have isolated a subunit of the Arp2/3 complex, Arc3, which binds proteasomes. When overexpressed, Arc3 rescues phenotypes associated with proteasome deficiencies; when its expression is repressed, proteasome deficiencies intensify. Arp2/3 is best known for regulating membrane dynamics and vesicular transport; thus, we performed photobleaching experiments and showed that proteasomes are readily imported into the nucleus but exit the nucleus slowly. Proteasome nuclear import is reduced when Arc3 is inactivated, leading to hypersensitivity to DNA damage and inefficient cyclin-B degradation, two events occurring in the nucleus. These data suggest that proteasomes display Arc3-dependent mobility in the cell, and mobile proteasomes can efficiently access substrates throughout the cell, allowing them to effectively regulate cell-compartment–specific activities.

INTRODUCTION

The 26S proteasome functions to degrade proteins that are marked by polyubiquitylation (Voges *et al.,* 1999). Ubiquitylated targets for proteasome degradation include proteins that are mis-folded due to abnormal protein synthesis or environmental assaults, as well as regulatory proteins whose timely removal is critical for proper transcription, signaling, and mitosis. As such, the 26S proteasome provides an indispensable machinery to remove damaged (and frequently cytotoxic) proteins and to maintain homeostasis of regulatory molecules.

Proteasome substrates may be produced throughout the cell. Moreover, some events that require proteasomal degradation, such as DNA damage repair, are restricted to a given cell compartment. What mechanisms must be in place so that proteasomes will always be available when a molecule anywhere in the cell needs to be promptly degraded? Is it possible that efficient proteolysis requires proteasomes to be highly mobile? If so, how is this mobility controlled?

Our lab has previously isolated the *yin6* gene in the fission yeast *Schizosaccharomyces pombe* during the study of Ras GTPase (Yen and Chang, 2000). *S. pombe yin6* is a homolog of the mammalian *INT6,* which was first discovered in a genetic screen using the mouse mammary tumor virus as an insertional mutagen to seek the *INT* genes that are important for breast tumor formation (Marchetti *et al.,* 1995; Sap and Chang, 2005). Int6/Yin6 can bind both proteasome and eIF3 subunits (thus it is also known as eIF3e/eIF3-p48; Asano *et al.,* 1997). In *S. pombe*, we have uncovered a key evolutionarily conserved role of Yin6, which is to interact with a Ras pathway to regulate the proteasome (Yen and Chang, 2003; Yen *et al.,* 2003b). In wild-type *S. pombe* cells, proteasomes concentrate at the nuclear membrane (Wilkinson *et al.,* 1998); in contrast, in *yin6* null (*yin6*Δ) cells, some proteasome subunits are improperly assembled or mislocalized in the cytoplasm or both.

To better understand how Yin6 influences proteasome functioning, we have conducted a high-copy suppressor screen to seek *S. pombe* cDNAs that when overexpressed rescue the growth defects in *yin6*Δ cells (Sha *et al.,* 2007). In the present study, we focus on one of the isolated cDNA clones, which encodes Arc3, a subunit of the Arp2/3 complex of actin regulatory proteins. Arc3 was chosen for further study for two key reasons: First, although there are two Ras pathways in *S. pombe*—the Byr2 MAPKK and the Cdc42 GTPase pathways,Yin6 selectively interacts with

This article was published online ahead of print in *MBoC in Press* (http://www.molbiolcell.org/cgi/doi/10.1091/mbc.E10–06–0506) on July 28, 2010.

‡ These authors contributed equally to this work.

Address correspondence to: Eric C. Chang (echang1@bcm.edu).

Abbreviations used: CHX, cyclohexamide; Lat A, latrunculin A; RI, relative intensity; Ub, ubiquitin.

the latter (Yen and Chang, 2000), which in many other organisms has been shown to regulate Arp2/3 (reviewed in Higgs and Pollard, 2001). Second, a ubiquitous function of the Arp2/3 complex is to promote actin polymerization to provide the force required for the budding and motility of COPI/COPII vesicles (Stamnes, 2002). We thus believe that this apparent link between Arc3 and proteasomes may shed light on the issues of whether proteasomes are mobile and whether mobile proteasomes are important for efficient proteolysis.

We report herein that Arc3, as well as other Arp2/3 subunits, are required for proper proteasome functioning in the cell. That is, overexpressing Arc3 rescues phenotypes of proteasome and *yin6* mutants, whereas repressing Arc3 expression intensifies proteasome mutant phenotypes and decreases the efficiency with which proteasomes function in the cell. Although Arc3 is required for efficient proteasome activity in the cell, no apparent defect in proteasome assembly and catalysis can be found when proteasomes are purified from Arc3-repressed cells. However, when Arc3 expression is silenced, proteasome nuclear import decreases, and cells become hypersensitive to DNA damage and inefficient in degrading cyclin-B, two events that occur in the *S. pombe* nucleus. These data suggest that high mobility is a critical property of the proteasome. Highly mobile proteasomes can rapidly reach every part of the cell to degrade proteins, and this property can reduce the need to transport potentially toxic molecules. Mobile proteasomes are also critical for efficiently regulating cellular events, e.g., DNA damage repair and mitosis that are cell-compartment restricted.

MATERIALS AND METHODS

Growth Conditions and Reagents

Cells were grown in either yeast extract (rich) medium (YEAU) or synthetic minimal medium (MM) with appropriate supplements (Chen *et al.*, 1999). To test for canavanine sensitivity, a stock solution of canavanine sulfate (50 mg/ml, Sigma, St. Louis, MO), was prepared in distilled water. To depolymerize F-actin, latrunculin A (Lat A) stock solution (1 mM, Sigma) was prepared in DMSO. To test sensitivity to DNA damage, phleomycin stock solution (5 mg/ml, Sigma) was prepared in DMSO. To repress the *nmt* promoters, thiamine was added from a 20 μM stock (Sigma) after autoclaving. To inhibit protein synthesis, a stock solution of cycloheximide (CHX; 100 mg/ml, Sigma) was prepared in DMSO. Plates spotted with cells were irradiated with UV in a 1800 UV Cross-linker (Stratagene, La Jolla, CA). We carried out all the experiments with cells pregrown to early logarithmic phase (2–5 $\times$ 10^6 cells/ml). For growth experiments on plates, cells were serially diluted 1:5.

Plasmid Constructions

pREP41GPIGFP was a kind gift from the Cande laboratory (University of California Berkeley) (Brazer *et al.*, 2000). Full-length *arc3* was amplified from an *S. pombe* cDNA library (Norbury and Moreno, 1997) and cloned into the BglII site of pSLF173 (Forsburg and Sherman, 1997) or the BamHI sites of pREP41 or pREP42 (Basi *et al.*, 1993), to generate pSLF173ARC3, pREP41ARC3, or pREP42ARC3, respectively. pSLF173 contains the strongest thiamine-repressible *nmt1* promoter, whereas pREP41 and pREP42 contain the medium strength *nmt* promoter (*nmt1**). The endogenous gene encoding ubiquitin (Ub; *ubi4*) in strain SP870 was tagged at its 3′ end with the coding sequence for green fluorescent protein (GFP) by homologous recombination using a PCR-based method (Janke *et al.*, 2004). The PCR primers were designed to also mutate the coding sequences of *ubi4* and GFP in order to create various mutant Ub-GFP fusion proteins. The first 70 nucleotides in these different forward primers anneal to *ubi4* and are all the same. Mutations were designed in the rest of the primers for creating different fusion proteins (Dantuma *et al.*, 2000). Primers GGT<u>ATG</u>GCT**AA**GTACGCTGCAGGTCGACGGATC, GGT<u>**AGA**</u>GCT**AA**GTACGCTGCAGGTCGACGGATC, and G**TT**<u>**GTA**</u>GCT**AA**GTACGCTGCAGGTCGACGGATC were used to generate M-GFP, R-GFP, and Ub^{G76V}-GFP. The codons for the first amino acid after Ub are underlined. The bold type marks those nucleotides that were changed to alter the coding sequence. We then performed PCR to amplify the coding sequences of various forms of Ub-GFP from the genomic DNA, digested them with BglII and SacI, and then cloned them into pRP (Onken *et al.*, 2006) to make pUBMGFP, pUBRGFP, and pUBVGFP, which express Ub-M-GFP, Ub-R-GFP, and Ub^{G76V}-GFP under the control of the *ras1* promoter, whose activity is fairly constant (Rustici *et al.*, 2004). In the former two Ub fusion proteins, the Ub was fused to GFP whose first amino acid residue is either a methionine or arginine. In the latter, the C-terminal glycine in the Ub moiety was mutated to valine. JP0DU was constructed by excising a BsrGI fragment inside *ura4* from KS-URA (JP0; Bähler *et al.*, 1998) and ligating the remaining fragment. To replace *yin6* with *ade6*, pBSYIN6g (Yen and Chang, 2000) was similarly digested to remove the coding sequence of *yin6*, and *ade6* was then inserted to create pYIN6A.

Strain Constructions

The parental wild-type *S. pombe* strain used in this study was SP870 (*h*^{90}, *ade6-M210, leu1–32, ura4-D18*) unless indicated otherwise. One copy of *arc3* was first deleted and replaced by the *ura4* selection marker in a SP870 diploid cells using homologous recombination via a PCR-based method (Bähler *et al.*, 1998). Correct gene replacement was confirmed by PCR. These *arc3::ura4*/+ cells were then transformed with pREP41ARC3, which expresses *arc3* from the *nmt1** promoter. Meiotic products from these cells were selected to carry both *arc3::ura4* and *nmt1*-arc3-LEU2*. The conditional *arc3* mutation so created was named *arc3*^{nmt}, and the mutant strain was named ARC3NMT. To disrupt the *ura4* marker gene in this strain, cells were transformed with HindIII-cut fragments of JP0DU, and *ura4*$^-$ cells were selected in MM supplemented with 0.1% 5-FOA. The resulting strain was named ARC3NLNMT. To further remove the *LEU2* marker, the strain ARC3NLNMT was transformed with pREP42ARC3 and grown for several generations in MM supplemented with leucine to facilitate the loss of *LEU2*, and we named the resulting cells ARC3NUNMT. On thiamine addition, these three *arc3*^{nmt} strains showed phenotypes identical to those reported with other Arp2/3 mutants (McCollum *et al.*, 1996; Morrell *et al.*, 1999). *arc3*^{nmt} *rpn11-gfp* cells were generated by crossing strain ARC3NMT with strain *rpn11-gfp* (Wilkinson *et al.*, 1998) followed by random spore selection. To analyze interaction between Arc3 and the proteasome by genetics, an *arc3*^{nmt} mutant (strain ARC3NLNMT) was crossed with the *mts4/rpn1*^{ts} mutant (Wilkinson *et al.*, 1997), followed by random spore selection. Multiple sets of wild-type, single, and double mutants were isolated to confirm that they display the same phenotypes. Similarly, the *rpn7*^{ts} mutant (Sha *et al.*, 2007) was crossed with the *arp2-1* mutant (Morrell *et al.*, 1999), and the tetratype tetrad was selected to isolate wild-type, *arp2-1*, *rpn7*^{ts}, and *rpn7*^{ts} *arp2-1* cells. Arc3 was tagged with 13$\times$ MYC at the C-terminus (*arc3-MYC*) by homologous recombination using PCR products from the pFA6a-13Myc-*hph* template (Sato *et al.*, 2005). Cells expressing Yin6-HA, Arc3-Myc, and 13G6-GFP (strain Y6HAA3MGGPI) were generated by crossing strain ECP21 (*yin6-HA*; Yen and Chang, 2000) with *arc3-myc* cells and random spore selection, followed by transformation with pREP4113G6GFP. Cells expressing Arc3-MYC and Rpn5-HA (strain A3MR5HA) were generated by tagging Arc3 with 13$\times$ MYC at the C-terminus in strain RPN5-HA (Yen *et al.*, 2003a). *rpn7*^{ts} *act1-48*, *rpn7-gfp act1-48*, and *rpn11-gfp act1-48* cells were generated by crossing *act1-48* cells (McCollum *et al.*, 1999) with either *rpn7*^{ts}, *rpn7-gfp* (Sha *et al.*, 2007), or *rpn11-gfp* (Wilkinson *et al.*, 1998) cells, followed by tetrad dissection. To create a *yin6::ade6* strain (strain YIN6A), SP870 cells were transformed by a linearized pYIN6A DNA fragment. α*4-gfp yin6*Δ cells were created by GFP-tagging α4 at the C-terminus in YIN6A strain via homologous recombination (Janke *et al.*, 2004). *cdc13-gfp arc3*^{nmt} and *rpn10/pus1:proA arc3*^{nmt} cells (strain A3NMT10PA) were generated by crossing *rpn10:proA* cells (Yen *et al.*, 2003b) and *Cdc13-gfp* cells with *arc3*^{nmt} cells and random spore selection. To generate *bub1*Δ*arc3*^{nmt} cells, strain (A21NLI) was crossed to a *bub1*Δ strain followed by random spore selection. The resulting double mutant was then crossed to cells expressing Cdc13-GFP. Cells expressing α4-YFP and Arc3-CFP were generated by homologous recombination using PCR products from plasmids pYM40 and pYM30 (Janke *et al.*, 2004). *cut8* was knocked out in *rpn7-gfp* cells (strain RPN7-GFP) using a ClonNat selection marker as described (Gregan *et al.*, 2006) to generate *cut8*Δ *rpn7-gfp* cells (strain N7GFPCUT8N).

Fluorescence Microscopy

To perform live cell imaging, cells were mounted on agar-embedding medium as described (Tran *et al.*, 2004). Samples were examined via an UPlanFI 100$\times$/1.30 NA oil objective on an Olympus BX61 microscope (Melville, NY), and the images were captured by either an ORCA ER (Hamamatsu, Bridgewater, NJ) or a Retiga 1300 (Q-Imaging, Austin, TX) camera. GFP levels were quantified using the Openlab software (Improvision, Lexington, MA). To measure the lifespan of Cdc13, stacks of three or eight images (at 0.5- or 1-μm intervals) were collected every minute for 1 h, during which focusing was readjusted every 15 min.

Photobleaching Data Acquisition

These studies were carried out by a Zeiss LSM510 confocal microscope with a Plan-Apochromat 63$\times$/1.4 NA oil objective equipped with an objective heater to maintain sample temperature at 30°C. A 25-mW argon laser was turned on at 75% of power. Images were all collected with the pinhole set at 10.42 airy units (AU) to maximize signal intensity, because yeast cells are small and the GFP signal dim. To measure the fluorescence intensity before photobleaching, the sample was scanned three times (4$\times$ zoom at 1% of laser power) and then 10 iterative laser pulses at full power were applied to the

nucleus to photobleach. For local nuclear fluorescence recovery after photobleaching (FRAP) experiments, four iterative laser pulses at full power were applied to photobleach, and this was followed by collecting 20 images at 500-ms intervals. Alternatively, local nuclear FRAP was also measured using a Leica TCS SP5 confocal microscope with a 63×/1.4 NA oil objective (Deerfield, IL). We did not find any appreciable difference in the mobility as measured by these two different instruments.

Photobleaching Data Analysis

All fluorescence intensity values were divided by the size of the area of interest (in pixels), and the final data were exported from the LSM software (Carl Zeiss) to Excel (Microsoft, Redmond, WA). The relative intensity (RI) in a region of interest was defined as: $RI = (I_t)/(I_0)$, where I_0 is the fluorescence intensity measured before photobleaching and I_t is the intensity measured at a given time point t. Both I_0 and I_t values are corrected for background noise by subtracting the intensity in a region that does not have any cell. In addition to the RI values of the photobleached samples, the RI in the nucleus of an unbleached cell in the same field was also measured to control for spontaneous photobleaching. For the calculation of recovery $\tau_{1/2}$ in local nuclear FRAP, the raw RI values were corrected for spontaneous photobleaching by dividing RI_B with RI_{UB} to yield $R_{IB/UB}$. The "Exponential Rise" model in Kaleidagraph software (Synergy Software, Reading, PA) was used to calculate the $\tau_{1/2}$. All $\tau_{1/2}$ values are expressed as average ± SEM.

Protein Half-Life Measurement

Cells were pregrown to early log phase at 30°C in the minimal medium to a cell concentration such that at the end of the experiment, the OD would be ≤0.5. After addition of 250 mM CHX, 20–50 ml of cells was harvested at each time point, and protein levels were measured by immunoblots.

Cell Fractionation

Microsomes were isolated as described (Movsichoff *et al.,* 2005) from strain Y6HAA3MGGPI. The lysates and the microsome and soluble fractions were analyzed by Western blots.

Immunoblotting

To detect ubiquitylated proteins and GFP, cells were lysed by glass beads in PBS (pH 7.4). *N*-ethylmaleimide (10 mM) was added in the lysis buffer to block cleavage of polyubiquitylated chains. Proteins were separated by standard SDS-PAGE and transferred to nitrocellulose membrane. To detect Ub and GFP, antibodies from Sigma (1:200) and Fitzgerald (1:1000; Concord, MA) were used. Proteasome subunits were analyzed by antibodies that detect Rpn10 (also known as Pus1; 1:1000), Rpn1 (also known as Mts4; 1:1000; Wilkinson *et al.,* 1997), and an anti-α subunits antibody (MCP231, 1:2000; BIOMOL, Plymouth Meeting, PA). A polyclonal rabbit antibody against the α4 subunit (1:500) is as described (Sha *et al.,* 2007). mAb 12CA5 (1:2000) was used to detect Rpn5-hemagglutinin (HA), and 9E10 was used to detect Arc3-Myc. An antibody against tubulin (TAT1; Woods *et al.,* 1989) was diluted 1:2000, and against β-actin 1:2000 (Abcam, Cambridge, MA). The anti Cdc8 antibody (1:1000) was a gift from M Balasubramanian (University of Singapore; Balasubramanian *et al.,* 1992). The anti-Arp3 antibody (1:1000) was a gift from Kathleen Gould (Vanderbilt University) (McCollum *et al.,* 1996). To quantify protein levels, fluorescently conjugated secondary antibodies were used, and the signals were measured by the Odyssey infrared imaging system (Li-Cor Biosciences, Lincoln, NE).

Chemical Cross-Linking

arc3-MYC rpn-5HA cells (strain A3MR5HA) were precultured in 1 l YEAU medium and then collected and washed before being resuspended in 5 ml of PBS containing 2 mM dithiobis[succinimidyl propionate (Thermo Scientific, Waltham, MA) for 2 h at 4°C. Cross-linking was terminated by adding 5 ml 20 mM Tris-Cl (pH 8.0) at room temperature for 15 min with rocking. Cells were then lysed by glass beads in lysis buffer (10 mM HEPES, pH 7.55, 150 mM NaCl, 0.5% sodium deoxycholate, 0.1% SDS, 1% IGEPAL CA-630, 1 mM PMSF, 10% glycerol, Complete Protease Inhibitor [Roche, Indianapolis, IN]). The lysate was then cleared by centrifugation, and immunoprecipitation was performed at 4°C overnight. Samples were analyzed by Western blots.

RESULTS

Arc3 Overexpression Rescues Proteasome Defects in yin6Δ Cells

To identify genes that regulate the proteasome, we screened an *S. pombe* cDNA library for genes that when overexpressed rescued the cold-dependent growth defects in *yin6*Δ cells. From this screen we isolated a full-length cDNA clone encoding a component of the Arp2/3 complex of actin regulatory proteins called Arc3. Arc3 carries a predicted molecular weight of 19.8 kDa and shares 51% identity with the human ARPC3 (actin-related protein 2/3 complex subunit 3; Welch *et al.,* 1997). We have shown previously that proteasome deficiencies cause *yin6*Δ cells to be hypersensitive to canavanine, an arginine analog, the incorporation of which results in the synthesis of abnormal proteins. Our results here show that Arc3 overexpression also rescued canavanine hypersensitivity in these cells (Figure 1A). Finally, we have shown that proteasomes are improperly mislocalized in cytoplasm in *yin6*Δ cells. To determine whether Arc3 overexpression can restore proteasome nuclear localization, we tagged one of the endogenous proteasome catalytic subunits α4 with GFP (Sha *et al.,* 2007) and then measured the ratio of α4-GFP signal in the cytoplasm versus the nucleus. As shown in Figure 1B, Arc3 overexpression modestly restored proteasome nuclear accumulation in *yin6*Δ cells (Figure 1B), such that relatively more α4-GFP could be detected in the nucleus of *yin6*Δ cells. These results indicate that the pro-

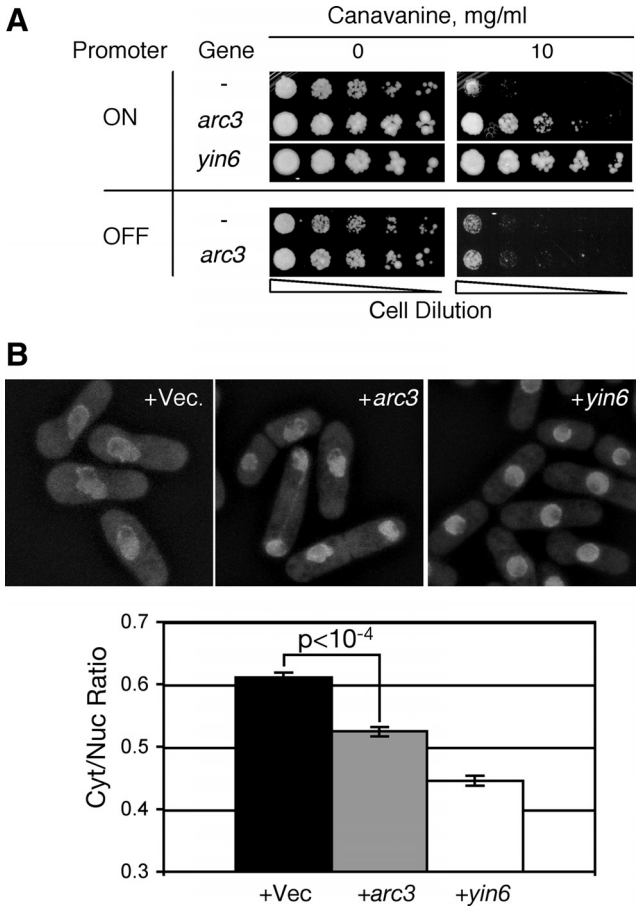

Figure 1. Arc3 overexpression rescues proteasome deficiencies of *yin6*Δ cells. (A) *yin6*Δ cells (strain YIN6A) were transformed with plasmids expressing *arc3* (pSLF173ARC3) or *yin6* (pHAYIN6; Yen and Chang, 2000) under the control of the thiamine-repressible *nmt1* promoter, or an empty vector (pSLF) as a control. Cells were pregrown in MM and serially diluted and spotted on MM plates with or without canavavine. Thiamine (20 μM) was used to turn off expression of the indicated gene. (B) *yin6*Δ α4-gfp cells were transformed with the same plasmids as in A. Transformed cells were reinoculated in fresh medium to grow to early log phase at 30°C before the signal of α4-GFP was quantified. The signal of α4-GFP in the cytoplasmic region versus the nucleus was measured and their ratio was plotted.

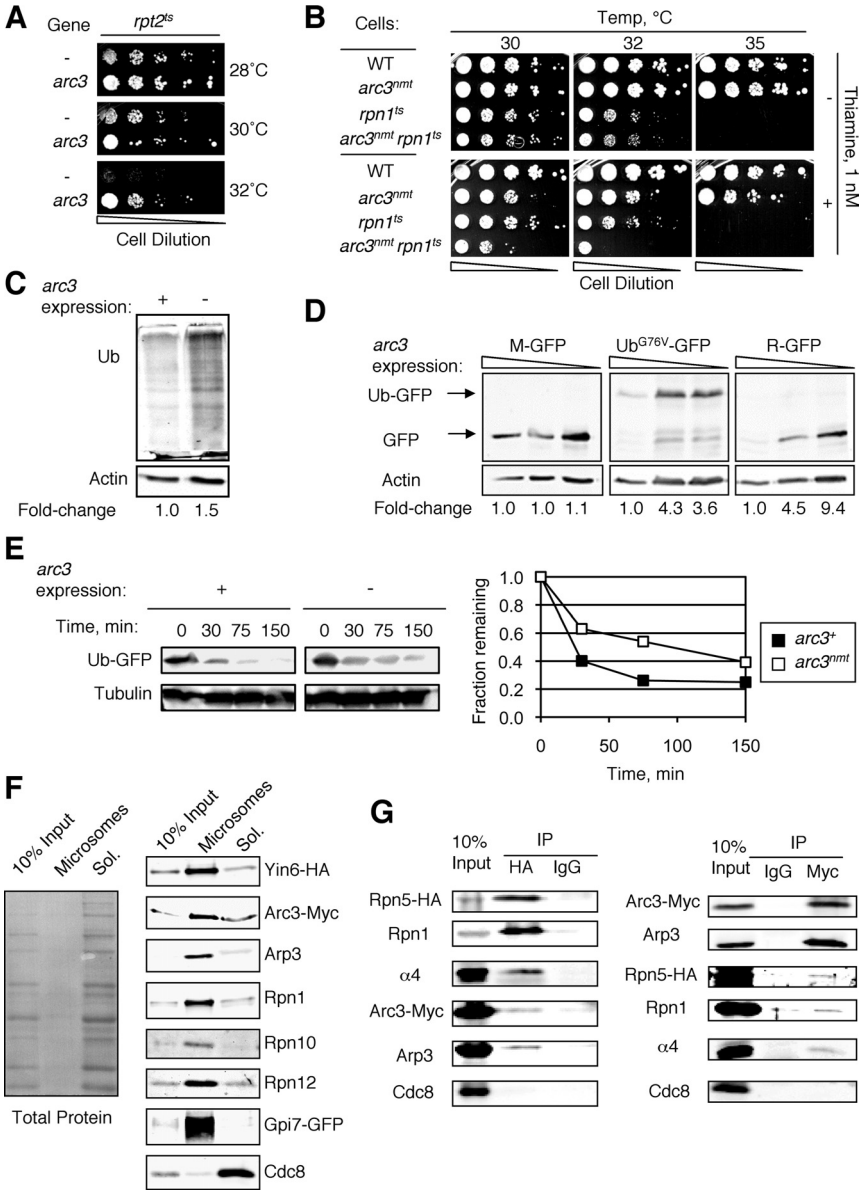

Figure 2. Arc3 is required for proper proteasome functioning. (A) *rpt2*^{ts} cells (Gordon *et al.,* 1993) were transformed with a plasmid expressing *arc3* (pSLF173ARC3), or an empty vector (pSLF) as control. Cells were serially diluted and grown on MM plates at indicated temperatures. (B) Cells were serially diluted and spotted on plates that either do not contain thiamine (top) or 1 nM thiamine (bottom) and then grown at indicated temperatures. The cells growing without thiamine had essentially normal Arc3 function, whereas 1 nM thiamine mildly repressed *arc3* expression. A synthetic growth defect in *arc3*^{nmt} *rpn1*^{ts} cells was evident at 32°C. (C) The *arc3*^{nmt} cells were precultured in MM medium at 30°C and then either untreated or treated with 200 nM thiamine for 20 h to suppress *arc3* expression. The levels of polyubiquitylated proteins were analyzed by Western blotting using an anti-Ub antibody. Actin was examined as a loading control. Polyubquitylated protein levels relative to the actin loading control were quantified, and this was set to 1 for control cells. (D) The *arc3*^{nmt} cells (strain ARC3NUMT) expressing the stable Ub-M-GFP or the unstable Ub^{G76V}-GFP and Ub-R-GFP fusion proteins were incubated with different concentrations of thiamine (0, 15, and 200 nM) to repress *arc3* expression at various levels, and cell lysates were analyzed by Western blots using antibodies against either GFP or the loading control actin. Note that the Ub of both Ub-M-GFP and Ub-R-GFP is readily cleaved off in the cell. GFP protein levels relative to the actin loading control were measured, and those were set to 1 in cells whose *arc3* was not repressed (bottom). (E) *arc3*^{nmt} cells expressing Ub^{G76V}-GFP were treated with or without thiamine as described in C, at t = 0, cycloheximide (CHX, 250 μM) was added, and time points were examined by Western blots. The fraction of Ub^{G76V}-GFP remaining is plotted on the right. (F) The microsomal fraction and the corresponding soluble fractions (Sol), along with the crude lysate input were prepared from cells expressing Yin6-HA, Arc3-Myc, and Gpi7-GFP (strain Y6HAA3MGGPI). Ponceau staining was used to detect total protein (left), and indicated proteins were revealed by Western blot (right). Whereas most proteins, including the actin regulatory protein Cdc8, are found in the soluble fraction, Yin6, many proteasome subunits, and the Arp2/3 complex are found predominantly in the microsomal fraction, along with the ER marker Gpi7. (G) *arc3-MYC rpn5-HA* cells were treated with the protein cross-linker DSP before the lysate was prepared for immunoprecipitation. The antibodies used in the immunoprecipitation (IP) experiment are as indicated, and the purified mouse IgG was the antibody control. The immunoprecipitated proteins were analyzed by Western blots using antibodies specific for proteins as indicated on the left.

teasome defects in *yin6*Δ cells are suppressed by Arc3 overexpression.

Arc3, as well as Other Arp2/3 Components, Is Required for Proper Proteasome Functioning in the Cell

Because Arc3 overexpression rescues proteasome defects in *yin6*Δ cells, we investigated using proteasome mutants whether Arc3 is required for proper proteasome functioning. First, our data in Figure 2A showed that Arc3 overexpression rescued the growth defect of the temperature-sensitive (ts) proteasome mutant carrying the *rpt2*^{ts}*/mts2-1* mutation (Gordon *et al.,* 1993). Next, we sought to inactivate Arc3. Like mutants lacking either *arp2* or *arp3* (Balasubramanian *et al.,* 1996; McCollum *et al.,* 1996; Morrell *et al.,* 1999), *arc3*Δ cells are inviable (*Materials and Methods*). We thus generated a strain carrying a conditional *arc3* mutation, which we call *arc3*^{nmt}. In this strain, the endogenous *arc3* has been replaced by an *nmt-arc3* cassette such that *arc3* expression is now under the control of the thiamine-repressible *nmt* promoter. We confirmed that when *arc3* expression was repressed, although there is no global disruption of F-actin structures, F-actin patches and cables become disorganized, as have been previously reported for other *arp2/3* mutants. This *arc3* mutation was crossed into a ts proteasome mutant carrying *mts4–288/rpn1*^{ts} (Wilkinson, 1997), and the resulting double mutants (Figure 2B) displayed severe growth defects under conditions that did not substantially impair the growth of either single mu-

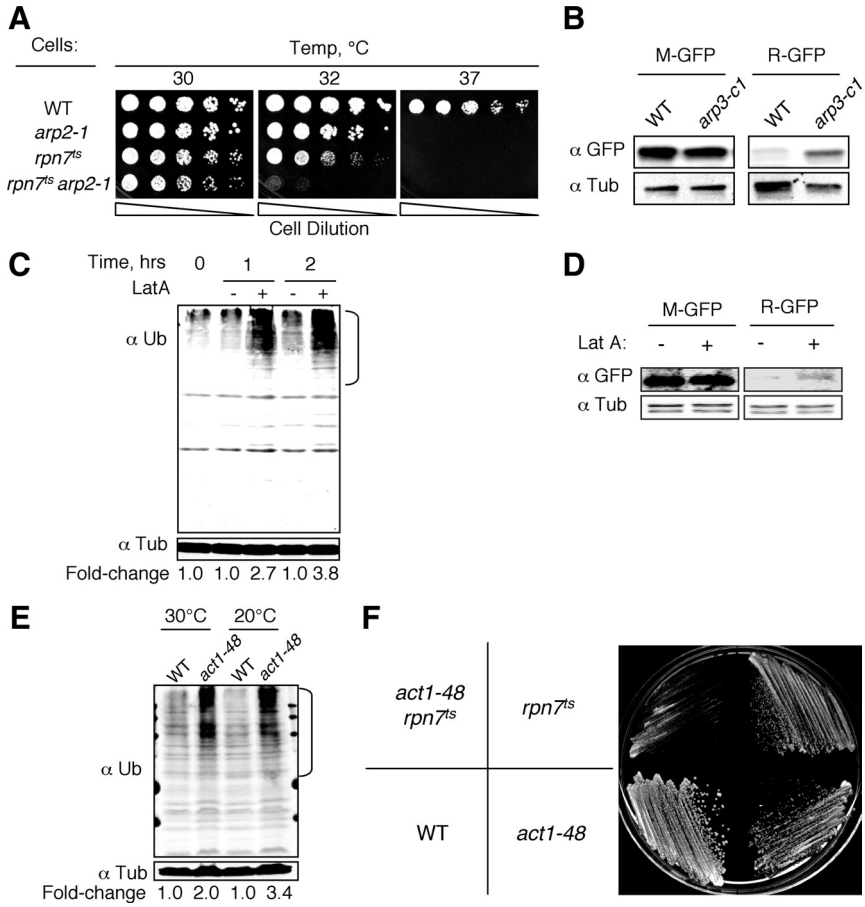

Figure 3. The Arp2/3 complex and F-actin are required for proper proteasome function. (A) Cells with the indicated genotypes were serially diluted and spotted on YEAU medium and grown at indicated temperatures. (B) Wild-type and *arp3*^{cs}*-1* cells expressing the M-GFP and R-GFP fusion proteins were incubated at 22°C, and the cell lysates were analyzed by Western blots. Tubulins were the loading control. (C) Wild-type cells were treated with Lat A (+, 10 μM) or DMSO alone (−) for 1 or 2 h, and Lat A was then washed out. Cell lysates were analyzed by Western blots using the indicated antibodies. The levels of polyubiquitylated proteins (marked by the bracket) relative to the tubulin loading control were quantified, and this was set to 1 at each time point for cells incubated in DMSO. (D) Wild-type cells expressing Ub-M-GFP or Ub-R-GFP were treated with cycloheximide (CHX, 250 μM, 1.5 h), with or without Lat A (10 μM, 1.5 h), and the cell lysates were analyzed by Western blots. (E) The *act1-48* mutant and the wild-type strain were pregrown at 30°C. Samples were taken before or after being shifted to 20°C for 7 h. Cell lysates were analyzed by Western blots using indicated antibodies. Polyubiquitylated proteins (marked by the bracket) relative to the tubulin loading control were quantified, and this value was set to 1 for wild-type samples at either temperature. (F) Cells with indicated genotypes were streaked on the same YEAU plate and grown at 30°C. Synthetic growth defects of *rpn7*^{ts} *act1-48* cells are shown by the inability to form colonies.

tant (e.g., at 32°C). Another ts proteasome mutation *rpn7*^{ts} (Sha *et al.*, 2007) was similarly tested with the same results (data not shown).

Inactivation of proteasomes can lead to accumulation of polyubiquitylated proteins. As shown in Figure 2C, levels of polyubiquitylated proteins increased in the *arc3*^{nmt} mutant cells. To more directly measure reduction in cellular proteasome activity, we constructed three Ub fusion proteins as reporters: Ub-M-GFP, Ub-R-GFP, and Ub^{G76V}-GFP (Dantuma *et al.*, 2000). Both Ub-M-GFP and Ub-R-GFP are cleaved after the Ub by endogenous Ub C-terminal hydrolases, and the resulting M-GFP is stable, with a half-life >6 h and thus can accumulate in wild-type cells (Supplemental Figure S1). In contrast, R-GFP and Ub^{G76V}-GFP are readily degraded by the proteasome via the N-end rule and Ub fusion degradation pathways, respectively. R-GFP and Ub^{G76V}-GFP have half-lives of 30 min and can only accumulate in cells with proteasome deficiency (Supplemental Figure S1 and data not shown). As shown in Figure 2D, both Ub^{G76V}-GFP and R-GFP, but not M-GFP, also accumulated in the *arc3*^{nmt} mutant cells, with a concurrent doubling in half-life (Figure 2E), indicating that Arc3 is required for efficient proteolysis in the cell.

Because Arc3 is an Arp2/3 complex subunit, we have similarly examined mutations in *arp2* and *arp3*. Our data showed that the ts *arp2-1* and the cold sensitive *arp3-c1* mutations (McCollum *et al.*, 1996) also intensified the phenotype of the proteasome *rpn7*^{ts} mutants (Figure 3A and data not shown). The *arp3-c1* mutant was further examined, and as shown in Figure 3B, R-GFP, but not M-GFP, accumulated to high levels in these cells. By contrast, two myosin mutants (*myo1* and *myp2*-Δ*2*; Bezanilla *et al.*, 1997; Lee *et al.*, 2000)) show no detectable accumulation of polyubiquitylated proteins (data not shown). Because Arp2/3 regulates the actin cytoskeleton, we treated wild-type cells with Lat A, which globally depolymerizes F-actin, and found that this induced accumulation of polyubiquitylated proteins (Figure 3C) and R-GFP (Figure 3D). Moreover, we examined the actin mutation *act1-48* (McCollum *et al.*, 1999); as shown in Figure 3E, it too caused accumulation of polyubiquitylated proteins and worsened the phenotype of the *rpn7*^{ts} mutant (Figure 3F). We conclude from these results that a functional Arp2/3 complex is required for proper proteasome activity in the cell.

Physical Interaction between Arc3 and Proteasomes

Arc3 and other Arp2/3 components appear as dots near the cell ends and cell equator; however, as much as 85% of the Arp2/3 components are not associated with these dots, but rather are diffused in the cytoplasm (Wu and Pollard, 2005). Conversely, although proteasomes are evidently concentrated at the nucleus, a substantial portion of them are also readily detectable in the cytoplasm. We performed laser confocal microscopy to analyze subcellular localization of a proteasome catalytic subunit, α4, tagged with YFP, and Arc3, tagged with CFP, and the data showed that they primarily colocalized in the cytoplasm (Supplemental Figure S2).

The Arp2/3 complex in mammalian cells is associated with the Golgi and cortical actin (Dubois *et al.*, 2005) and is best known for its role in mediating intracellular pro-

tein trafficking between Golgi and ER (e.g., by controlling vesicle formation and maintenance of structural integrity in these membrane organelles). Furthermore, proteasomes have been shown to concentrate in the microsomal fractions, which are enriched with ER and Golgi, as well as other internal membrane structures, of budding yeast (Elkabetz *et al.*, 2004). We thus analyzed whether in *S. pombe* Arc3 and proteasomes cofractionate in the microsomal fractions. Our data showed that indeed Arc3, as well as at least one other Arp2/3 subunit, Arp3, cofractionated with Yin6 and many proteasome subunits in the microsome fractions, and they evidently cofractionated with the ER-membrane protein Gpi7 (Figure 2F). In contrast, another actin regulatory protein, Cdc8 (tropomyosin), was enriched in the soluble fraction. Finally, we tested whether the proteasome and Arp2/3 proteins form a complex by immunoprecipitation using cells in which endogenous Arc3 and Rpn5 were both epitope-tagged by homologous recombination. Our data show that when Rpn5-HA was immunoprecipitated, in addition to several proteasome subunits (Rpn1 and the catalytic proteasome subunit α4), Arc3-Myc, as well as Arp3, was also found brought down by Rpn5-HA (Figure 2G). Conversely, when Arc3-Myc was immunoprecipitated, Rpn5-HA and other protesome subunits coprecipitated with it. In contrast, Cdc8 was not detected in the pull-downs. These data support the idea that the Arp2/3 complex interacts with and regulates proteasomes mostly in regions rich with internal membranes.

Normal Levels and Catalytic Activity of Proteasomes Purified from the Arc3 Mutant

Because proteasomes inefficiently degrade their substrates in the *arc3* mutant cells, we first examined proteasome subunit levels in crude cell lysate and found that they were not decreased in the *arc3*^{nmt} mutant ("input", Supplemental Figure S3A). We then purified proteasomes by pulling down the proteasome subunit Pus1/Rpn10 and found that there was no detectable change in the levels of copurified proteasome subunits (Supplemental Figure S3A). Furthermore, when the purified proteasomes were measured in vitro for the ability to cleave the model substrate Suc-LLVY-AMC, they appeared to be as active as those from wild-type cells (Supplemental Figure S3B). In agreement with this notion, we found that proteasomes from the *arc3* mutant cells were able to degrade a recombinant polyubiquitylated protein Sic1 in vitro as efficiently as those from wild-type cells did (Supplemental Figure S3C). These data suggest that when *arc3* levels are down-regulated, proteasomes are still properly assembled and retain their full catalytic activity when measured in vitro.

Efficient Nuclear Import of Proteasomes

One of the best-documented functions of the Arp2/3 complex is to mediate cellular transport and maintain proper membrane structures. Therefore, we investigated whether proteasomes are mobile and whether Arc3 and the actin cytoskeleton play any role in controlling their mobility.

Proteasomes can be found in both the cytoplasm and nucleus in many different cell types. In *S. pombe*, proteasomes accumulate to high levels at the nuclear membrane. How this pattern is established is not entirely clear. We thus performed photobleaching experiments to examine Rpn11, a proteasome regulatory subunit, which when tagged with GFP via homologous recombination is incorporated into proteasomes and fully functional (Wilkinson *et al.*, 1998). To measure nuclear import, we photobleached the entire nuclei of cells carrying Rpn11-GFP and then measured over time the reappearance of the GFP signal in the nucleus. Conversely, to measure nuclear export, the entire cytoplasm was photobleached, and the fluorescence recovery in the cytoplasm was then measured. Control experiments were performed to photobleach the whole cell to reveal that during the course of these experiments, no new proteasome synthesis was detected (Supplemental Figure S4A). Our data showed that proteasome nuclear entry was at least threefold more efficient than proteasome nuclear exit (Figure 4A). We examined another proteasome regulatory subunit, Rpn7, and obtained the same result (Figure 4B and Sha *et al.*, 2009). One leading model suggests that proteasomes are anchored in the nucleus by Cut8 (Tatebe and Yanagida, 2000). Cut8 is thus expected to affect the nuclear export of proteasomes. Indeed, in *cut8*Δ cells, proteasome nuclear export was nearly as efficient as import (Figure 4B). We conclude that these photobleaching experiments are effective in analyzing proteasome trafficking in and out of the nucleus, demonstrating that proteasomes are efficiently imported into the nucleus and are held back from exiting by Cut8.

Proteasome Nuclear Import Mediated by Arc3

We then investigated whether functional Arc3 and the actin cytoskeleton are required for efficient proteasome nuclear import as measured above. As shown in Figure 4C, although Rpn11-GFP accumulation at the nuclear membrane was observed within 15 min in wild-type cells, it was not detectable until 45 min when *arc3* expression was silenced. At 45 min, Rpn11-GFP already accumulated to high levels inside the nucleus in control cells, whereas none was detectable in the *arc3*-repressed cells.

The actin cytoskeleton may be necessary for maintaining the integrity of the nuclear pore complex because the Arp2/3 complex has been shown to regulate the function of the nuclear pore (Yan *et al.*, 1997). To investigate whether disrupting the actin cytoskeleton may globally disrupt nuclear pore functions, we examined nuclear import of a model cargo, GLFE (Yoshida and Sazer, 2004), in cells treated with Lat A but detected no difference in its import into the nucleus (Supplemental Figure S5A). This suggests that the nuclear pore is functional in the absence of F-actin. This result also demonstrates that F-actin depolymerization does not globally block transport of all proteins in the cell.

Intranuclear Proteasome Mobility Modulated by Arc3

During the course of photobleaching nuclear proteasomes, we noted that when a small area of the nucleus of cells expressing Rpn11-GFP was photobleached, Rpn11-GFP from the surrounding area in the nucleus quickly moved to the bleached area, yielding a recovery $\tau_{1/2}$ of 1.31 ± 0.03 s (Figure 5A). Rpn7 and a catalytic subunit, α4, were similarly measured, and the same results were obtained ($\tau_{1/2}$ = 1.46 ± 0.05 and 1.35 ± 0.05 s, respectively). Furthermore, this mobility also requires functional Arc3: it was reduced when Arc3 expression was reduced (Figure 5D), and it was increased when Arc3 was overexpressed (Figure 5E). Consistent with the fact that Arc3 is part of the actin cytoskeleton, Lat A (Figure 5B) and the presence of the *act1-48* mutation (Figure 5C) both reduced proteasome mobility without affecting those of Cut11-GFP, R-GFP, and M-GFP (data not shown). These results demonstrate that inactivating Arc3, as well as F-actin, selectively inhibits proteasome nuclear mobility. It seems that Arc3 and the actin cytoskeleton are not only needed

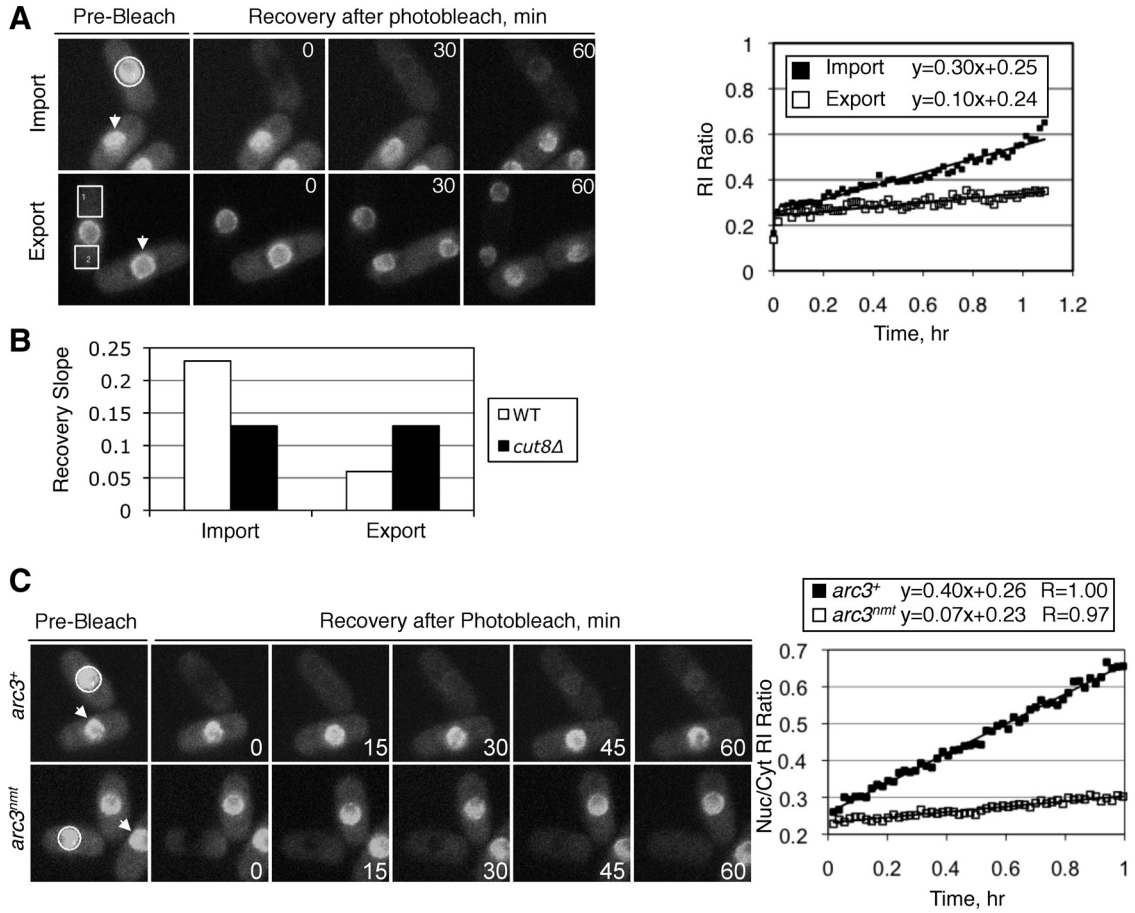

Figure 4. Proteasomes nuclear import requires Arc3. (A) To measure nuclear import (top, left), the laser was targeted to the entire nucleus of a selected cell (white circle), and fluorescence recovery in that nucleus was recorded over time. The arrow marks the nucleus of an unbleached cell whose fluorescence levels were measured to correct for spontaneous photobleaching. To quantify nuclear import (right), we calculated the RI corrected for spontaneous photobleaching at each time point after photobleaching and plotted the ratio of nuclear versus cytoplasmic RI over time (■). To measure export (bottom, left), two areas (square 1 and 2) in the cytoplasm were simultaneously photobleached. The cell marked by an arrow was taken as the control for measuring spontaneous photobleaching. On the right, the ratio of cytoplasmic to the nuclear corrected RI was plotted (□). These import/export experiments were performed three times, and the RI values were averaged. The data sets that estimate the efficiencies of nuclear import ($RI_{N/C}$) and export ($RI_{C/N}$) can be fitted to trendlines (inset) with r values of 0.97 and 0.84, respectively. (B) The same experiment as in A was performed on wild-type and *cut8*Δ cells expressing Rpn7-GFP (strain RPN7GFP and N7GFPCUT8N, respectively), and RI ratio lines were generated as in A. (C) Whole nucleus photobleaching experiments similar to A were performed on *arc3^{nmt} rpn11-gfp* cells, whose expression of *arc3* was repressed as in Figure 2E. The laser-targeted nucleus is marked by a white circle, and the arrow head marks the nucleus of an unbleached cell whose fluorescence levels were measured to correct for spontaneous photobleaching. On the right, nuclear import was quantified for *arc3*$^{+}$ cells (□) or *arc3^{nmt}* cells (■) as in A.

to efficiently deliver proteasomes into the nucleus, they also play a role maintaining proteasomes in a highly mobile state in the nucleus.

Mobile Proteasomes Are Required for DNA Damage Repair and Normal Anaphase in the Nucleus

In budding yeast, proteasomes are critical for repairing DNA double-strand breaks induced by UV and bleomycin (Krogan *et al.*, 2004). Intriguingly, *S. pombe cut8* mutant cells, whose proteasomes do not efficiently accumulate in the nucleus, are also defective in DNA damage repair (Kearsey *et al.*, 2007). Furthermore, *cut8* mutants are inefficient in degrading cyclin-B (encoded by *cdc13*) during anaphase (Tatebe and Yanagida, 2000), which like DNA damage control, occurs in the nucleus. These observations support the idea that proteasomes must move and accumulate in the nucleus in order to regulate DNA damage repair and anaphase progression. We confirmed that proteasome and *yin6* mutants in *S. pombe* are also hypersensitive to a compound related to bleomycin, phleomycin (Figure 6A). Intriguingly, this abnormality was more pronounced in the cold, a condition that retards protein mobility. In addition to phleomycin, we also used UV to induce DNA damage and obtained the same results (Figure 6B). Next, we ascertained whether the Arc3-mediated proteasome mobility and/or nuclear import are important for DNA damage repair. As shown in Figures 6, the *arc3^{nmt}* mutant cells were also hypersensitive to both phleomycin and UV at cold temperatures. Consistent with the fact that Arp2/3 regulates actin polymerization, the *act1-48* mutant is similarly sensitive to phleomycin and UV (Figures 6, A and B). These data support the hypothesis that Arp2/3 complex–mediated actin polymerization is required to import proteasomes in sufficient quantities to carry out DNA damage repair.

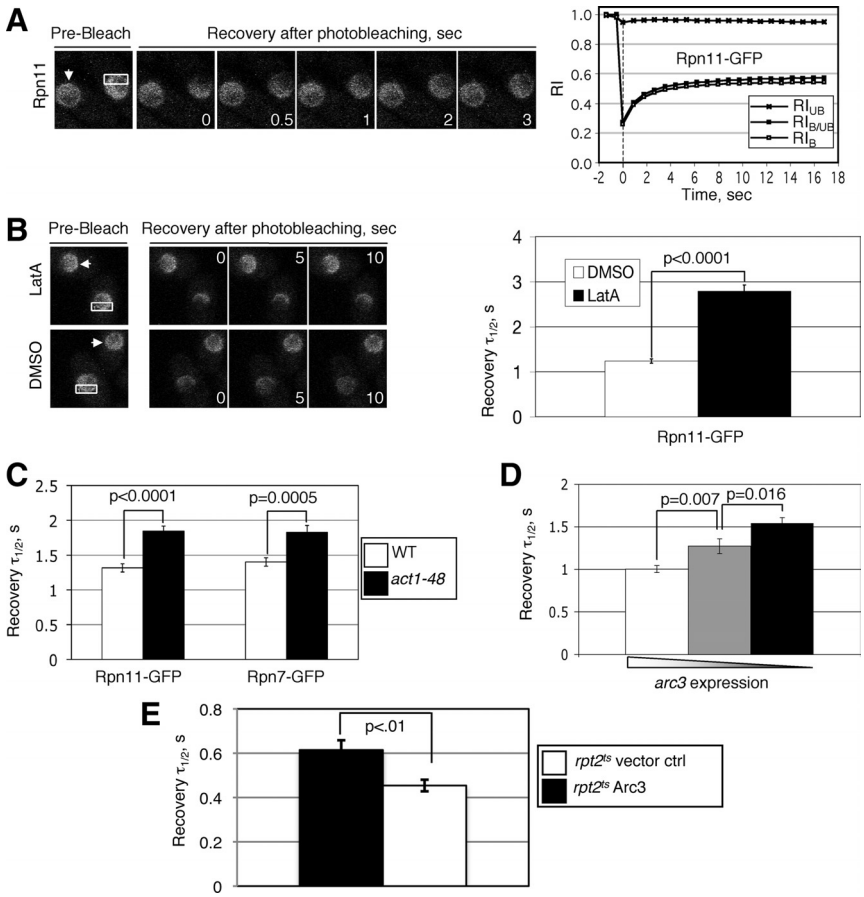

Figure 5. Intranuclear proteasome mobility requires Arc3. (A) Photobleaching was performed on *rpn11-gfp* cells. On the left, images of cells before and after photobleaching (rectangle) were captured over time. We plotted the relative fluorescence intensity of Rpn11-GFP either in the photobleached region (RI_B, open squares) or in the nucleus of an adjacent unbleached cell (arrow; RI_{UB}, crosses) over time. RI_B was further divided by RI_{UB} to generate $RI_{B/UB}$ value (closed squares) to correct for spontaneous photobleaching. Because there was no measurable spontaneous photobleaching, the RI_B and $RI_{B/UB}$ curves overlap extensively. The recovery $\tau_{1/2}$ is 1.31 ± 0.03 (n = 100) s. We note that the recovery does not reach the initial GFP intensity at t = 0. This is because once one region of the nucleus was photobleached, the signal in the rest of the nucleus also diminished because of high mobility. This is evident in the figure and confirmed by FLIP experiments, in which one side of the nucleus was repeatedly photobleached while the loss of fluorescence in the other side of the nucleus was recorded (data not shown). (B) Photobleaching experiments similar to that in A were performed on *rpn11-gfp* cells that were treated with either Lat A (20 μM, 1 h) or the DMSO control. Representative time course images are shown on the left. The photobleached region is marked by a rectangle, and the nucleus of the unbleached control cell is marked by an arrow. The average recovery $\tau_{1/2}$ is shown on the right. n = 25. (C) Photobleaching experiments similar to those in A were performed for Rpn11-GFP and Rpn7-GFP in wild-type or *act1-48* cells. n = 25. (D) Photobleaching experiments similar to A were performed on *arc3*^{nmt} *rpn11-gfp* cells, whose expression of *arc3* was repressed as in Figure 2E. n = 25. (E) The *rpt2*^{ts} cells stably expressing Rpn7-GFP were transformed with either the vector control (pSLF173) or a vector overexpressing Arc3 (pSLF173ARC3), and photobleaching experiments similar to those in A were performed. n = 10.

In *S. pombe*, cyclin-B/Cdc13 associates with the spindle at the onset of prometaphase in the nucleus and must later be degraded by the proteasome to facilitate anaphase progression. We performed live-cell time-lapse microscopy to measure the lifespan of cyclin-B/Cdc13 on the spindle in a strain whose endogenous Cdc13 is tagged by GFP (Tatebe and Yanagida, 2000). We defined the onset of prometaphase as the time point at which two Cdc13-GFP dots (attached to the just separated spindle pole bodies) were first detected (Figure 6E), and our results showed that repressing *arc3* expression markedly prolonged Cdc13-GFP life span on the spindle. This delay in cyclin-B degradation does not seem to involve activation of the spindle checkpoint because it also occurs in cells deleted for the checkpoint kinase *bub1* (Figure 6E). Note that the effect of the mutation on Cdc13 degradation is quite selective. For instance, in both the *arc3*^{nmt} mutant and control cells the Cdc13 levels on the spindle at t = 0 were approximately the same, suggesting that *arc3* deficiency did not detectably affect Cdc13 movement into the nucleus. Furthermore, their anaphase B (elongation of nuclear membrane, Figure 6E) started with the same delay after Cdc13 degradation, suggesting that the silencing of *arc3* expression did not substantially impair the onset of anaphase B.

We conclude that highly mobile proteasomes make it possible to efficiently degrade proteins throughout the cell and that their entry into the nucleus is critical for controlling DNA damage repair and anaphase progression.

DISCUSSION

Through the cloning of Arc3 as a high copy suppressor for *yin6*Δ cells, we have been able to address an intriguing and important issue: are proteasomes stationary or mobile in order to efficiently degrade their substrates throughout the cell? Our data show that increasing Arc3 levels rescues the phenotype of proteasome mutants; conversely, decreasing Arc3 levels reduces proteolysis efficiency and intensifies the phenotype of proteasome mutants. Despite the fact that proteasomes are not efficient in the cell when *arc3* expression is repressed, when these proteasomes are examined in vitro after purification, they appear to be properly assembled and as active as those from normal cells. Because components of the Arp2/3 complex are frequently implicated in mediating protein and organelle trafficking and maintaining internal membrane integrity, and our data show that Arp2/3 and proteasome subunits interact with the microsomal membrane fraction, we investigated whether proteasomes are mobile and whether this mobility is regulated by Arc3. We demonstrated by photobleaching that proteasomes are efficiently imported into the nucleus. When Arc3 is inactivated proteasome entry into the nucleus is substantially blocked, leading to inefficient DNA damage repair and delayed cyclin-B degradation, two events occurring in the nucleus.

Arc3 is a subunit of the Arp2/3 complex of actin regulatory proteins. Consistent with this, we show that other subunits in the Arp2/3 complex are also required for proper proteasome

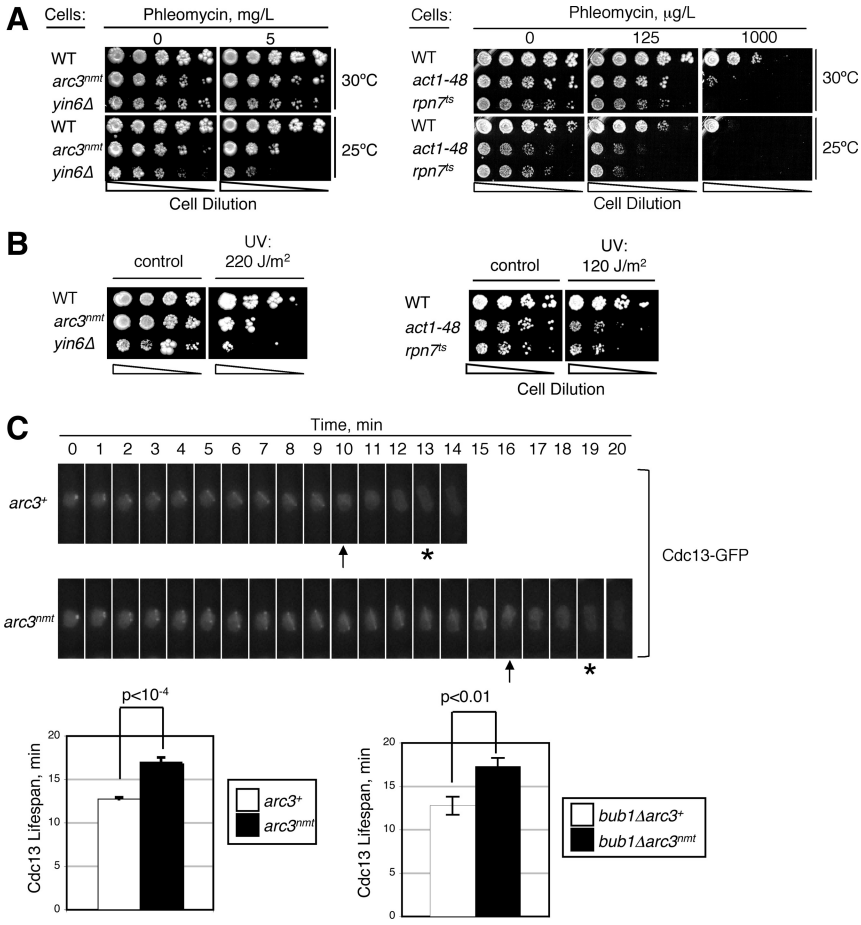

Figure 6. Mobile proteasomes are required for DNA damage repair and normal anaphase in the nucleus. (A) Cells of the indicated genotypes were serially diluted and spotted on plates containing the rich (YEAU) medium (right) or minimal medium containing 1 nM thiamine (to repress *arc3* expression, left) with or without the DNA-damaging agent phleomycin and then incubated at the indicated temperatures. Note that these cells were much less sensitive to phleomycin in minimal medium; thus, more phleomycin was used on the plates shown on the left. (B) Cells of the indicated genotypes were serially diluted and spotted on YEAU medium (right) or minimal medium plates containing 1 nM thiamine (to repress *arc3* expression, left) and irradiated with the indicated dose of UV radiation. Cells were incubated at 28°C (left) and 30°C (right). (C) The $arc3^{nmt}$ cells expressing *cdc13-gfp* were pretreated with 200 nM thiamine for 16 h ($arc3^{nmt}$) or untreated ($arc3^{+}$). These cells were examined by time-lapse microscopy with deconvolution (top). To measure the life span of Cdc13 on the spindle, t = 0 was defined as the onset of separation of the spindle pole bodies, to which Cdc13-GFP was attached, and the end point was when Cdc13-GFP disappeared from the spindle (marked by arrows). The *bub1* gene was deleted in these cells, and the Cdc13 life span was measured similarly (n = 37). Note that once Cdc13 was degraded, these cells initiated anaphase B (elongation of the nuclear membrane, asterisk) normally within 3–4 min.

functions; in contrast, the two examined myosins are not. Because Arp2/3 regulates the actin cytoskeleton, disruption of F-actin by Lat A or actin mutations also impair proteasome function. In contrast, disruption of microtubule functions by the presence of the *mal3*Δ mutation (Beinhauer *et al.*, 1997) or by adding MBC (methyl benzimidazolecarbamate) does not impede proteasome mobility (data not shown). Our data also show that abnormal actin quite selectively affects the mobility of proteasomes but not that of Cut11 and the model substrates M-GFP and R-GFP. These results argue against the possibility that the observed inhibition in proteasome mobility is due to nonspecific depolymerization of cytoskeletal components. Therefore, although we cannot rule out that Arc3 and actin can influence the movement of other molecules necessary for proteolysis, we strongly argue that the mobility of the proteasome itself is a critical factor for efficient proteolysis. Collectively our data support the model that proteasome mobility and activity in the cell are selectively regulated at least in part by the Arp2/3 complex.

Why do proteasomes need to be so mobile? Because many proteasome substrates may be toxic to the cell, highly mobile proteasomes can reduce the need to transport their substrates over long distances, thus reducing exposure to these toxic molecules. Furthermore, because the coordinated interactions between an E3 Ub ligase, a proteasome, and a substrate might render that particular proteasome temporarily unavailable for processing another substrate, high proteasome mobility could serve to assure efficient delivery of proteasomes to that area. Finally, many biological processes are cell-compartment restricted. Beside DNA damage repair and Cdc13/cyclin-B degradation, we have shown previously that proteasome mutants contain abnormal V- or star-shape spindles (Yen *et al.*, 2003a), suggesting that nuclear proteasomes are also needed for proper spindle formation. In addition, the roles of proteasomes in transcription are well recognized (Collins and Tansey, 2006). In short, mobile proteasomes can thus move quickly to the appropriate compartment such as the nucleus in order to properly control these events.

The Arp2/3 complexes serve as nuclei for promoting actin polymerization to form branched meshwork structures. This mode of actin polymerization is frequently catalyzed by members of the WASP (Wiskott-Aldrich syndrome protein) family, which can bind cell membranes and recruit the Arp2/3 complex to promote F-actin polymerization, providing the force and/or structural rigidity needed in remodeling the membrane for motility (e.g., the formation of lamellipodia) and transport (e.g., vesicle fission and movement and motility of organelles, such as mitochondria). Consistent with the idea that Arp2/3 is expected to associate with membrane fractions, our data indicate that the majority of Arc3 and Arp3, as well as proteasome subunits, are found in the microsomal fractions and that they form a complex with proteasomes. These results suggest that Arp2/3 interacts with proteasomes in endomembrane compartments. Mass spectrometry analyses have shown that in budding yeast Arp2 can bind two proteasome subunits (Ho *et al.*, 2002), and with cross-linking, three more Arp2/3 subunits, including Arc18, the budding yeast Arc3 homolog, have been found to copurify with proteasomes (Guerrero *et al.*, 2008). We note that cross-linking is also needed to detect the binding between Arc3 and proteasomes in *S. pombe*, suggesting that the

interaction between Arp2/3 and proteasomes is transient in many eukaryotes. We note that additional actin-dependent mechanisms may be operative to enhance the efficiency of compartmentalized proteolysis in *S. pombe*. For example, a recent study shows that the class V myosin Myo52 in *S. pombe* cooperates with the Ub receptor Dph1 to regulate Tip1 degradation at the cell tips (Martin-Garcia and Mulvihill, 2009), suggesting that Ub receptors and/or E3s may be transported in a myosin–actin-dependent manner to a given cell compartment.

Although the underlying mechanism regulating proteasome mobility is likely to be very complex, one possibility is that proteasomes can associate with vesicles to be transported to different cell compartments. In support of this idea, proteasomes in mammalian cells have been shown to associate with endosomes, ER, and the ER-Golgi intermediate compartment via ECM29 (Gorbea *et al.*, 2004). In budding yeast, Guerrero *et al.* (2008) showed that Sec26, Sar1, several other vesicle coat components, and many Arp2/3 subunits copurified with budding yeast proteasomes. In a recent article of ours, using LC-MS/MS, we found that proteasomes associate with translation factors and other proteins in a supercomplex, called translasome (Sha *et al.*, 2009). In that study, we also found Sar1 and Sec26 in the translasome. In agreement with the idea that proteasomes may be imported into the nucleus via the cellular trafficking system, our ongoing study shows that expression of a dominant-negative Sar1 similarly impaired proteasome nuclear import (unpublished results).

Subunits in a large protein complex are expected to interact in a stoichiometric manner. It is thus quite intriguing that overexpressing Arc3 can rescue mutant phenotypes. However, we and others have observed similar phenomena when we studied the proteasomes whose subunits are well known to interact stoichiometrically. For example, we have shown that overexpression of *S. pombe* proteasome subunits Rpt2 and Rpn12 rescues the phenotypes of *rpn5*Δ cells (Yen *et al.*, 2003a). In addition, *S. pombe yin6*Δ cells contain mis-assembled proteasomes, but the mutant phenotype can be rescued by overexpressing many proteasome subunits, Rpn5, Rpt2, Rpn11, Rpn1, and Rpn7 (Yen *et al.*, 2003b; Sha *et al.*, 2009). Similar results were obtained in budding yeast and human cells (Kominami *et al.*, 1998; Chondrogianni *et al.*, 2005). One possible explanation is that increased abundance of individual subunits may drive more efficient assembly of the complex. Alternatively, certain subunits may not be present in stoichiometric amounts and may act as limiting factors for the complex.

Activities proposed to require nuclear actin have intrigued many researchers because they include functions critical for cell physiology, such as transcription, chromatin remodeling, and the trafficking of RNA and ribosomes. Arp2/3, in particular, has been shown to mediate nuclear actin polymerization required for the replication of a baculovirus in insect cells (Goley *et al.*, 2006). Moreover the activator for Arp2/3, WASP, has been implicated in RNA polymerase I– and II–dependent transcription (Fomproix and Percipalle, 2004; Philimonenko *et al.*, 2004). The observation that proteasomes are also mobile inside the nucleus in a partially Arc3-dependent manner suggests that proteasome mobility may be a new activity controlled by the nuclear actin cytoskeleton. How the nuclear actin cytoskeleton can regulate these activities is unclear primarily because no F-actin structure has ever been fully resolved in the nucleus.

We suggest that actin-dependent proteasome mobility may be evolutionarily conserved in mammalian cells. The mammalian dendritic spines in neurons are enriched with the Arp2/3 complex, which is also required for the formation of these dendritic spines (Wegner *et al.*, 2008). It has been shown recently that 26S proteasomes rapidly translocate from the dendritic shafts to the spines within a few minutes after neuron depolarization (Bingol and Schuman, 2006). Although the Arp2/3/actin cytoskeleton was not directly demonstrated in that study to regulate the movement of the proteasomes, the neuronal proteasomes do associate with F-actin after depolarization. It would be interesting to determine whether such proteasome translocation is also similarly mediated by Arp2/3. Reits *et al.* (1997) examined the mobility of the immuno-proteasome by fluorescence loss in photobleaching (FLIP) using a GFP-tagged subunit βli/LMP2 that was ectopically expressed in HT1080 fibrosarcoma cells. Immuno-proteasomes are structurally unique and function specifically for antigen presentation. Despite this, they too observed that the rate of proteasome nuclear import is greater than that of nuclear export. However using sodium azide, Reits *et al.* concluded that the immuno-proteasomes move within the nucleus and within the cytoplasm in an ATP-independent manner, implying that they move entirely by passive diffusion in HT1080 cells. It is possible that different proteasomes in different cells can move by different mechanisms. Moreover, Reits *et al.* measured proteasome mobility by detecting the loss of GFP levels after photobleaching at a single time point. This approach might not have detected the change in the rate of fluorescence loss. Finally, ATP depletion may affect the assembly of these proteasomes, a possibility that can complicate the interpretation of mobility data. We conclude that actin-dependent 26S proteasome movement is evolutionarily conserved; however, different proteasomes may move by different mechanisms, which may be further influenced by cell type.

ACKNOWLEDGMENTS

We thank Jeannie Zhong, Irina Larina, and Michael Mancini for their superb assistance in microscopy. We thank Keith Gull (Oxford University), Dan McCollum (University of Massachusetts), Fred Chang (Columbia University), Mitsuhiro Yanagida (Kyoto University), Chuan-wei Jang (University of Texas), Minoru Yoshida (RIKEN), and Jian-Qiu Wu (Yale University) for providing materials critical for this study, and Gary Chamness, Shelly Sazer, Jeannette Kunz, Xiangwei He, Mike Lewis, and Adrian Lee at Baylor College of Medicine, and Stan Gorski at National Institutes of Health (NIH) ,National Cancer Institute for helpful discussions. We also thank Glen and Judy Smith for their generous support. E.C.C. is supported by grants from the NIH (CA90464 and CA107187) and the Susan G. Komen Foundation (PDF0402733); Z.S. is supported by a predoctoral fellowship from the Department of Defense (BC030443).

REFERENCES

Asano, K., Merrick, W. C., and Hershey, J. W. (1997). The translational initiation factor eIF3–p48 subunit is encoded by *int6*, a site of frequent integration by the mouse mammary tumor virus genome. J. Biol. Chem. *272*, 23477–23480.

Bähler, J., Wu, J. Q., Longtine, M. S., Shah, N. G., McKenzie, A., 3rd, Steever, A. B., Wach, A., Philippsen, P., and Pringle, J. R. (1998). Heterologous modules for efficient and versatile PCR-based gene targeting in *Schizosaccharomyces pombe*. Yeast *14*, 943–951.

Balasubramanian, M. K., Feoktistova, A., McCollum, D., and Gould, K. L. (1996). Fission yeast Sop2p: a novel and evolutionarily conserved protein that interacts with Arp3p and modulates profilin function. EMBO J. *15*, 6426–6437.

Balasubramanian, M. K., Helfman, D. M., and Hemmingsen, S. M. (1992). A new tropomyosin essential for cytokinesis in the fission yeast *S. pombe*. Nature *360*, 84–87.

Basi, G., Schmid, E., and Maundrell, K. (1993). TATA box mutations in the *Schizosaccharomyces pombe nmt1* promoter affect transcription efficiency but not the transcription start point or thiamine repressibility. Gene *123*, 131–136.

Beinhauer, J. D., Hagan, I. M., Hegemann, J. H., and Fleig, U. (1997). Mal3, the fission yeast homologue of the human APC-interacting protein EB-1 is required for microtubule integrity and the maintenance of cell form. J. Cell Biol. *139*, 717–728.

Bezanilla, M., Forsburg, S. L., and Pollard, T. D. (1997). Identification of a second myosin-II in *Schizosaccharomyces pombe*: Myp2p is conditionally required for cytokinesis. Mol. Biol. Cell *8*, 2693–2705.

Bingol, B., and Schuman, E. M. (2006). Activity-dependent dynamics and sequestration of proteasomes in dendritic spines. Nature *441*, 1144–1148.

Brazer, S. C., Williams, H. P., Chappell, T. G., and Cande, W. Z. (2000). A fission yeast kinesin affects Golgi membrane recycling. Yeast *16*, 149–166.

Chen, C. R., Li, Y. C., Chen, J., Hou, M. C., Papadaki, P., and Chang, E. C. (1999). Moe1, a conserved protein in *Schizosaccharomyces pombe*, interacts with a Ras effector, Scd1, to affect proper spindle formation. Proc. Natl. Acad. Sci. USA *96*, 517–522.

Chondrogianni, N., Tzavelas, C., Pemberton, A. J., Nezis, I. P., Rivett, A. J., and Gonos, E. S. (2005). Overexpression of proteasome beta5 assembled subunit increases the amount of proteasome and confers ameliorated response to oxidative stress and higher survival rates. J. Biol. Chem. *280*, 11840–11850.

Collins, G. A., and Tansey, W. P. (2006). The proteasome: a utility tool for transcription? Curr. Opin. Genet. Dev. *16*, 197–202.

Dantuma, N. P., Lindsten, K., Glas, R., Jellne, M., and Masucci, M. G. (2000). Short-lived green fluorescent proteins for quantifying ubiquitin/proteasome-dependent proteolysis in living cells. Nat. Biotechnol. *18*, 538–543.

Dubois, T., Paleotti, O., Mironov, A. A., Fraisier, V., Stradal, T. E., De Matteis, M. A., Franco, M., and Chavrier, P. (2005). Golgi-localized GAP for Cdc42 functions downstream of ARF1 to control Arp2/3 complex and F-actin dynamics. Nat. Cell Biol. *7*, 353–364.

Elkabetz, Y., Shapira, I., Rabinovich, E., and Bar-Nun, S. (2004). Distinct steps in dislocation of luminal endoplasmic reticulum-associated degradation substrates: roles of endoplasmic reticulum-bound p97/Cdc48p and proteasome. J. Biol. Chem. *279*, 3980–3989.

Fomproix, N., and Percipalle, P. (2004). An actin-myosin complex on actively transcribing genes. Exp. Cell Res. *294*, 140–148.

Forsburg, S. L., and Sherman, D. A. (1997). General purpose tagging vectors for fission yeast. Gene *191*, 191–195.

Goley, E. D., Ohkawa, T., Mancuso, J., Woodruff, J. B., D'Alessio, J. A., Cande, W. Z., Volkman, L. E., and Welch, M. D. (2006). Dynamic nuclear actin assembly by Arp2/3 complex and a baculovirus WASP-like protein. Science *314*, 464–467.

Gorbea, C., Goellner, G. M., Teter, K., Holmes, R. K., and Rechsteiner, M. (2004). Characterization of mammalian Ecm29, a 26 S proteasome-associated protein that localizes to the nucleus and membrane vesicles. J. Biol. Chem. *279*, 54849–54861.

Gordon, C., McGurk, G., Dillon, P., Rosen, C., and Hastie, N. D. (1993). Defective mitosis due to a mutation in the gene for a fission yeast 26S protease subunit. Nature *366*, 355–357.

Gregan, J., Rabitsch, P. K., Rumpf, C., Novatchkova, M., Schleiffer, A., and Nasmyth, K. (2006). High-throughput knockout screen in fission yeast. Nat. Protoc. *1*, 2457–2464.

Guerrero, C., Milenkovic, T., Przulj, N., Kaiser, P., and Huang, L. (2008). Characterization of the proteasome interaction network using a QTAX-based tag-team strategy and protein interaction network analysis. Proc. Natl. Acad. Sci. USA *105*, 13333–13338.

Higgs, H. N., and Pollard, T. D. (2001). Regulation of actin filament network formation through ARP2/3 complex: activation by a diverse array of proteins. Annu. Rev. Biochem. *70*, 649–676.

Ho, Y., *et al.* (2002). Systematic identification of protein complexes in *Saccharomyces cerevisiae* by mass spectrometry. Nature *415*, 180–183.

Janke, C., *et al.* (2004). A versatile toolbox for PCR-based tagging of yeast genes: new fluorescent proteins, more markers and promoter substitution cassettes. Yeast *21*, 947–962.

Kearsey, S. E., Stevenson, A. L., Toda, T., and Wang, S. W. (2007). Fission yeast Cut8 is required for the repair of DNA double-strand breaks, ribosomal DNA maintenance, and cell survival in the absence of Rqh1 helicase. Mol. Cell. Biol. *27*, 1558–1567.

Kominami, K., Seth-Smith, H., and Toda, T. (1998). Apc10 and Ste9/Srw1, two regulators of the APC-cyclosome, as well as the CDK inhibitor Rum1 are required for G1 cell-cycle arrest in fission yeast. EMBO J. *17*, 5388–5399.

Krogan, N. J., *et al.* (2004). Proteasome involvement in the repair of DNA double-strand breaks. Mol. Cell *16*, 1027–1034.

Lee, W. L., Bezanilla, M., and Pollard, T. D. (2000). Fission yeast myosin-I, Myo1p, stimulates actin assembly by Arp2/3 complex and shares functions with WASp. J. Cell Biol. *151*, 789–800.

Marchetti, A., Buttitta, F., Miyazaki, S., Gallahan, D., Smith, G., and Callahan, R. (1995). Int-6, a highly conserved, widely expressed gene, is mutated by mouse mammary tumor virus in mammary preneoplasia. J. Virol. *69*, 1932–1938.

Martin-Garcia, R., and Mulvihill, D. P. (2009). Myosin V spatially regulates microtubule dynamics and promotes the ubiquitin-dependent degradation of the fission yeast CLIP-170 homologue, Tip1. J. Cell Sci. *122*, 3862–3872.

McCollum, D., Balasubramanian, M., and Gould, K. (1999). Identification of cold-sensitive mutations in the *Schizosaccharomyces pombe* actin locus. FEBS Lett. *451*, 321–326.

McCollum, D., Feoktistova, A., Morphew, M., Balasubramanian, M., and Gould, K. L. (1996). The *Schizosaccharomyces pombe* actin-related protein, Arp3, is a component of the cortical actin cytoskeleton and interacts with profilin. EMBO J. *15*, 6438–6446.

Morrell, J. L., Morphew, M., and Gould, K. L. (1999). A mutant of Arp2p causes partial disassembly of the Arp2/3 complex and loss of cortical actin function in fission yeast. Mol. Biol. Cell *10*, 4201–4215.

Movsichoff, F., Castro, O. A., and Parodi, A. J. (2005). Characterization of *Schizosaccharomyces pombe* ER alpha-mannosidase: a reevaluation of the role of the enzyme on ER-associated degradation. Mol. Biol. Cell *16*, 4714–4724.

Norbury, C., and Moreno, S. (1997). Cloning cell cycle regulatory genes by transcomplementation in yeast. Methods Enzymol. *283*, 44–59.

Onken, B., Wiener, H., Philips, R. M., and Chang, E. C. (2006). Compartmentalized signaling of Ras in fission yeast. Proc. Natl. Acad. Sci. USA *103*, 9045–9050.

Philimonenko, V. V., *et al.* (2004). Nuclear actin and myosin I are required for RNA polymerase I transcription. Nat. Cell Biol. *6*, 1165–1172.

Reits, E. A., Benham, A. M., Plougastel, B., Neefjes, J., and Trowsdale, J. (1997). Dynamics of proteasome distribution in living cells. EMBO J. *16*, 6087–6094.

Rustici, G., Mata, J., Kivinen, K., Lio, P., Penkett, C. J., Burns, G., Hayles, J., Brazma, A., Nurse, P., and Bahler, J. (2004). Periodic gene expression program of the fission yeast cell cycle. Nature Genetics *36*, 809–817.

Sap, J., and Chang, E. C. (2005). Int6. AfCS-Nature Molecule Pages (doi: 10.1038/mp.a003493.01).

Sato, M., Dhut, S., and Toda, T. (2005). New drug-resistant cassettes for gene disruption and epitope tagging in *Schizosaccharomyces pombe*. Yeast *22*, 583–591.

Sha, Z., Brill, L. M., Cabrera, R., Kleifeld, O., Scheliga, J. S., Glickman, M. H., Chang, E. C., and Wolf, D. A. (2009). The eIF3 interactome reveals the translasome, a supercomplex linking protein synthesis and degradation machineries. Mol. Cell *36*, 141–152.

Sha, Z., Yen, H.-c.S., Scheel, H., Suo, J., Hofmann, K., and Chang, E. C. (2007). Isolation of the *Schizosaccharomyces pombe* proteasome subunit Rpn7 and a structure-function study of the PCI domain. J. Biol. Chem. *282*, 32414–32423.

Stamnes, M. (2002). Regulating the actin cytoskeleton during vesicular transport. Curr. Opin. Cell Biol. *14*, 428–433.

Tatebe, H., and Yanagida, M. (2000). Cut8, essential for anaphase, controls localization of 26S proteasome, facilitating destruction of cyclin and cut2. Curr. Biol. *10*, 1329–1338.

Tran, P. T., Paoletti, A., and Chang, F. (2004). Imaging green fluorescent protein fusions in living fission yeast cells. Methods *33*, 220–225.

Voges, D., Zwickl, P., and Baumeister, W. (1999). The 26S proteasome: a molecular machine designed for controlled proteolysis. Annu. Rev. Biochem. *68*, 1015–1068.

Wegner, A. M., Nebhan, C. A., Hu, L., Majumdar, D., Meier, K. M., Weaver, A. M., and Webb, D. J. (2008). N-wasp and the arp2/3 complex are critical regulators of actin in the development of dendritic spines and synapses. J. Biol. Chem. *283*, 15912–15920.

Welch, M. D., DePace, A. H., Verma, S., Iwamatsu, A., and Mitchison, T. J. (1997). The human Arp2/3 complex is composed of evolutionarily conserved subunits and is localized to cellular regions of dynamic actin filament assembly. J. Cell Biol. *138*, 375–384.

Wilkinson, C. R., Wallace, M., Morphew, M., Perry, P., Allshire, R., Javerzat, J. P., McIntosh, J. R., and Gordon, C. (1998). Localization of the 26S proteasome during mitosis and meiosis in fission yeast. EMBO J. *17*, 6465–6476.

Wilkinson, C. R., Wallace, M., Seeger, M., Dubiel, W., and Gordon, C. (1997). Mts4, a non-ATPase subunit of the 26 S protease in fission yeast is essential for mitosis and interacts directly with the ATPase subunit Mts2. J. Biol. Chem. *272*, 25768–25777.

Wilkinson, K. D. (1997). Regulation of ubiquitin-dependent processes by deubiquitinating enzymes. FASEB J. *11*, 1245–1256.

Woods, A., Sherwin, T., Sasse, R., MacRae, T. H., Baines, A. J., and Gull, K. (1989). Definition of individual components within the cytoskeleton of *Trypanosoma brucei* by a library of monoclonal antibodies. J. Cell Sci. *93*, 491–500.

Wu, J. Q., and Pollard, T. D. (2005). Counting cytokinesis proteins globally and locally in fission yeast. Science *310*, 310–314.

Yan, C., Leibowitz, N., and Melese, T. (1997). A role for the divergent actin gene, ACT2, in nuclear pore structure and function. EMBO J. *16*, 3572–3586.

Yen, H.-c.S., and Chang, E. C. (2000). Yin6, a fission yeast Int6 homolog, complexes with Moe1 and plays a role in chromosome segregation. Proc. Natl. Acad. Sci. USA *97*, 14370–14375.

Yen, H. C., and Chang, E. C. (2003). INT6, A link between the proteasome and tumorigenesis. Cell Cycle *2*, 81–83.

Yen, H. C., Espiritu, C., and Chang, E. C. (2003a). Rpn5 is a conserved proteasome subunit and required for proper proteasome localization and assembly. J. Biol. Chem. *278*, 30669–30676.

Yen, H. C., Gordon, C., and Chang, E. C. (2003b). *Schizosaccharomyces pombe* Int6 and Ras homologs regulate cell division and mitotic fidelity via the proteasome. Cell *112*, 207–217.

Yoshida, M., and Sazer, S. (2004). Nucleocytoplasmic transport and nuclear envelope integrity in the fission yeast *Schizosaccharomyces pombe*. Methods *33*, 226–238.